analytical chemistry

Article

pubs.acs.org/ac

Wide Linear-Range Detecting Nonenzymatic Glucose Biosensor Based on CuO Nanoparticles Inkjet-Printed on Electrodes

Rafiq Ahmad,[†] Mohammad Vaseem,[†] Nirmalya Tripathy,[†] and Yoon-Bong Hahn*[,†,‡]

[†]Department of BIN Fusion Technology, School of Semiconductor and Chemical Engineering, Chonbuk National University, 567 Baekje-daero, Deokjin-gu, Jeonju 561-756, Republic of Korea

[‡]Nanomaterials Processing Research Center, Chonbuk National University, 567 Baekje-daero, Deokjin-gu, Jeonju 561-756, Republic of Korea

ABSTRACT: Inkjet-printed copper oxide nanoparticles (CuO NPs) on silver electrodes were used to fabricate the nonenzymatic glucose biosensor. The inkjet-printed CuO NPs electrodes produced high and reproducible sensitivity of 2762.5 μAm M^{-1} cm^{-2} at an applied potential of +0.60 V with the wide linear-detecting range of 0.05−18.45 mM and the detection limit of ~0.5 μM (S/N = 3). The long-term stability and reproducibility of sensor in glucose electrooxidation resulted from the chemical stability of CuO NPs and pore-like structure formed on Ag surface, which prevented the CuO NPs from conglomeration and the interference of oxygen in the air. Significantly, the effect of interfering species, such as AA, UA, and DA were negligible, whereas sugar derivatives (lactose, fructose, and mannose) show insignificant interference. Finally, the electrode was applied to analyze glucose concentration in human serum samples.

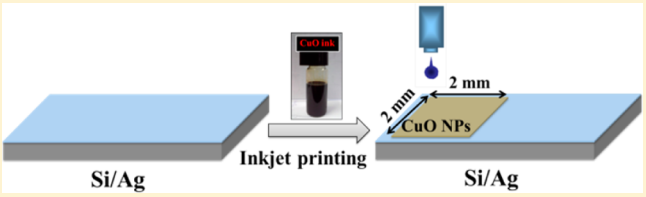

For the development of electrochemical glucose sensor, the electrodes are modified with glucose oxidase (GOx) to use in many areas such as clinical and industrial applications.[1−6] However, there are some disadvantages of the enzyme-modified electrodes, for instance, the instability of the electrode and unsatisfactory reproducibility, the immobilization procedure is complicated, and the enzymes are expensive and easily lose activation. Therefore, it is important to develop novel electrode materials with high sensitivity and stability and that are interference-free in glucose nonenzymatic determination. As an important p-type semiconductor metal oxide with a narrow band gap (1.2 eV), copper oxide (CuO) with virtue of natural abundance, low production cost, good electrochemical and catalytic properties is of particular interest, which makes it suitable for the application in electrical, optical and photovoltaic devices,[7,8] heterogeneous catalysis,[9,10] magnetic storage media,[11] gas sensing,[12,13] field-emission emitters,[14] lithium ion electrode[15] materials, and so forth. The shape and dimensions of the nanomaterial have a great influence on their properties.[16−19]

However, there is a challenge to research a method to attach these nanostructures onto a certain solid support (electrode) and keep their morphology, so that same kind of nanostructure can be available in the applications. Recently, inkjet-printing technique to fabricate semiconductor as well as conductive devices is considered as a most promising technology by which device fabrication can be possible via direct and simple steps without wasting processing materials.[20−24] In inkjet printing technology, the basic requirement is to formulate ink using nanoparticles, which must be well suited for inkjet printer heads (nozzles).

In this paper, we report for the first time, the nonenzymatic glucose biosensors based on CuO NPs inkjet-printed on the Si/Ag electrodes under ambient conditions. The electrochemical activities of the electrodes toward glucose were studied in alkaline electrolyte. It shows better sensing properties than those from other morphological CuO nanostructures integrated on the different working electrodes (gold, platinum, etc.) by using cross-linkers or sol−gel process. The inkjet printed CuO NPs are highly porous, having large surface area and forms tight adhesion with the Si/Ag working electrode. Thus, printed CuO NPs provides an efficient strategy for the development of low-cost working electrodes by drop-on-demand printing and chip-on-demand assembly for highly stable and better performing sensors.

EXPERIMENTAL DETAILS

Reagents. Copper acetate dihydrate [Cu-$(CH_3COO)_2.2H_2O$], sodium hydroxide (NaOH, 96% purity), acetic acid, ethanol, isopropanol, ethylene glycol, glucose (D-(+)-99.5%), ascorbic acid, L-cysteine, uric acid, lactose, mannose, fructose, dopamine, citric acid, sodium citrate, NaCl, KH_2PO_4 and human blood serum (H4522) were purchased from Sigma-Aldrich. All the chemicals were used as received without further purification. Ultrapure water purified with Milli-Q plus system (Millipore Co.) was exclusively used in all aqueous solutions and rinsing procedure

Received: August 2, 2013
Accepted: September 26, 2013
Published: September 26, 2013

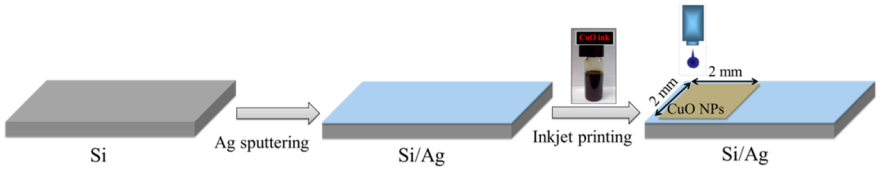

Figure 1. Schematic illustration of a procedure to fabricate inkjet-printed Si/Ag/CuO NPs working electrode for nonenzymatic electrochemical sensor.

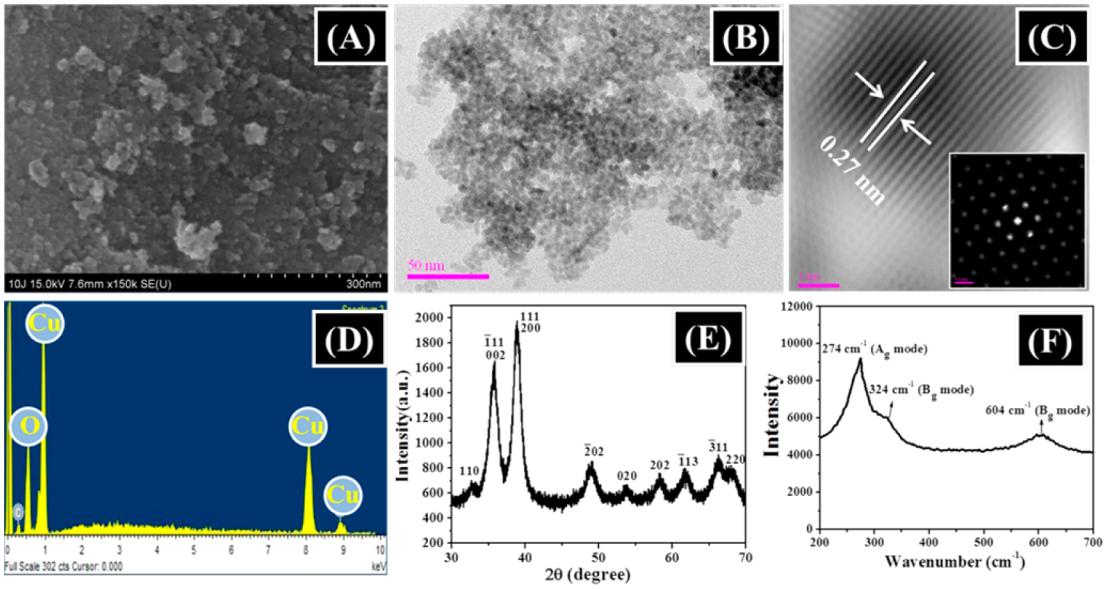

Figure 2. (A) FESEM, (B) TEM, and (C) high-resolution TEM images, (D) EDS spectrum, (E) typical XRD pattern, and (F) Raman-scattering spectrum of as-synthesized CuO NPs. The inset in panel C shows SAED pattern.

with resistivity ~18 MΩ cm. The electrochemical measurements were performed in 0.10 mM NaOH electrolyte.

Synthesis of CuO NPs. In a typical synthesis process, 100 mL of 0.02 M copper acetate solution is mixed with 0.50 mL acetic acid and then slowly heated in a three-necked refluxing pot under stirring. When the temperature reached at 90 °C, 0.50 g of NaOH was added, which resulted in black color solution (pH = 5−6) indicating the formation of CuO NPs. In this reaction condition, the NaOH acts as a basic source and the acetic acid breaks the precipitates for the formation of uniform and disperse CuO NPs. After 10−15 min refluxing, black-colored colloidal solution was obtained, followed by centrifugation at 3000 rpm for 2 min and washing with deionized water and ethanol.

Ink-Formulation and Printing. The as-synthesized CuO NPs were formulated as an ink using mixed solvents of deionized water, ethanol, isopropyl alcohol, and ethylene glycol in the ratio of 50:20:5:5 vol%. The ink formulation and jetting properties were discussed in detail in our previous studies.[25] The CuO NPs concentration in the solution was adjusted as 20 wt %. The resulted solution was then stirred for 24 h. The formulated CuO ink was then filtered by 0.45 μm polypropylene (PP) whatman paper before jetting. The observed viscosity of as-formulated inks was 4.14 cP using spindle speed of 200 rpm and shear rate of 264 s^{-1} at room temperature. The surface tension of as-prepared ink sample was 35.426 mN/m. For the fabrication of sensor (Figure 1), first a thin layer of Ag (~100 nm) was sputtered on the Si substrate. Then the CuO NPs ink was directly printed on Si/Ag substrates using drop-on-demand piezoelectric inkjet nozzle (manufactured by Dimatix) with diameter of 16 μm and drop volume was 10 pL. Uniform and continuous ejection of droplets was achieved by adjusting various wave-forms while applying firing voltage of 40 V at a 40 kHz printer velocity. The jetting velocity of ejected droplets was ~3.3 m/s. The cartridge print height was ~0.30 mm. The number of overprinting layers controlled the thickness of as-printed films and film uniformity was controlled by varying drop spacing (DS). Postannealing treatment of the as-printed CuO film was performed by microwave-assisted annealing (MAA) for 2 min.

Apparatus and Electrochemical Measurements. The structural investigation of as-synthesized CuO NPs was carried out by field emission scanning electron microscopy (FESEM, Hitachi S4700), transmission electron microscopy (TEM) equipped with digital charge-coupled device (JEOL-JEM-2010 equipped with CCD camera). Crystallinity of the CuO NPs was examined by X-ray diffraction (XRD, Rigaku) with Cu Kα radiation (λ = 1.54178 Å) in the range of 30−70° at 40 kV. The single crystallinity and chemistry of the as-grown NPs were examined with selected area electron diffraction (SAED) and energy-dispersive X-ray spectroscopy (EDS), respectively. The chemical structure of the CuO NPs was analyzed using atomic force microscopy (AFM). The viscosity of the CuO NPs ink was characterized by LVDV-II+Pro Viscometer (Brookfield). The cyclic voltammetry (CV) and amperometric measurements were carried out using an electrochemical analyzer connected to a personal computer. All experiments were carried out using a conventional three-electrode system with the Si/Ag/CuO NPs as the working electrode, a platinum wire as the counter electrode, and Ag/AgCl with saturated KCl solution as the

dx.doi.org/10.1021/ac402925r | Anal. Chem. 2013, 85, 10448−10454

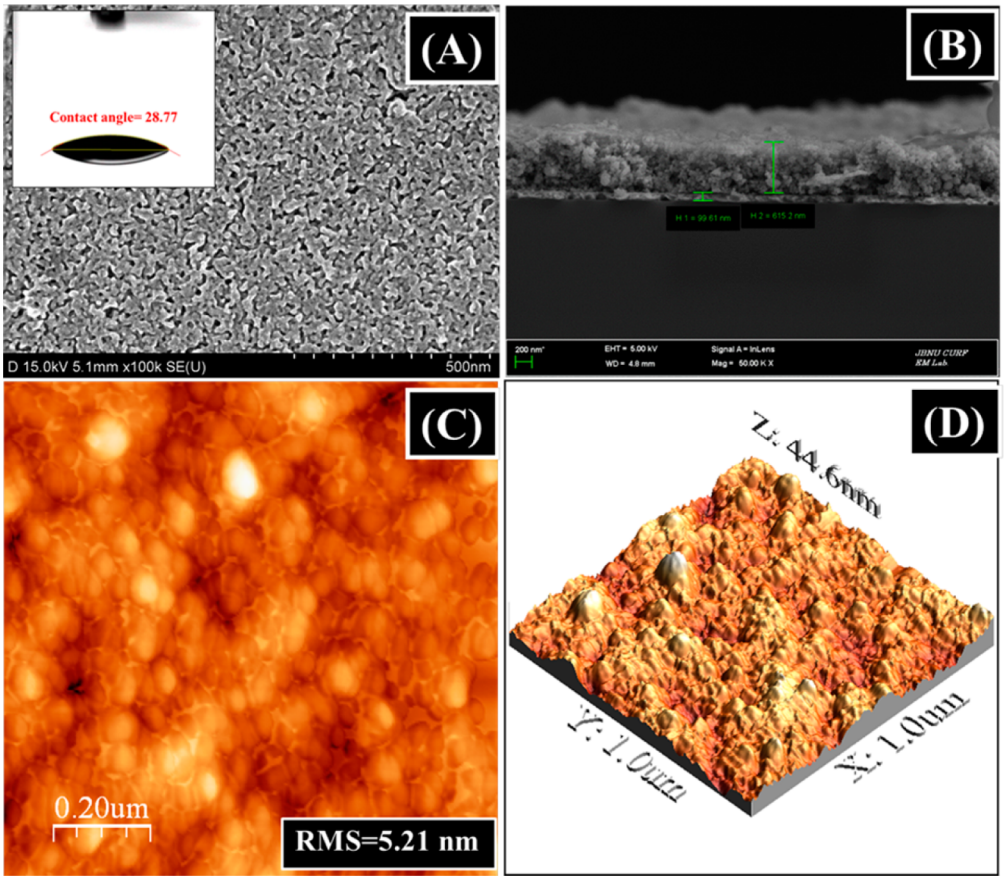

Figure 3. (A) Surface, (B) cross-sectional FESEM, and (C, D) AFM images of as-printed CuO nanofilms on Si/Ag substrate after Microwave-assisted annealing for 2 min. The inset in (A) shows contact angle of droplets using as-formulated CuO ink on Si/Ag substrate.

reference electrode. All the potentials in this work were measured with respect to Ag/AgCl reference electrode and the electrochemical measurements were carried out at room temperature in 0.10 M NaOH. Each cyclic voltammetry was performed in a solution of 20 mL volume between 0 and +0.80 V (vs Ag/AgCl). In steady state amperometric experiments, the potential was set at +0.60 V vs Ag/AgCl electrode with magnetic stirring.

RESULTS AND DISCUSSION

Structural and Optical Properties of CuO NPs. Figure 2 shows the FESEM image (A), TEM image (B), and HR-TEM image (C) of CuO NPs, respectively. The CuO NPs are of spherical shape and uniformly grown in a high density with average diameter of ∼5−8 nm. From HR-TEM the distance between two neighboring lattice fringes was measured as 0.27 nm, which corresponds to the [110] lattice fringe of the monoclinic CuO. Its corresponding SAED pattern confirmed the single crystallinity of as-grown CuO NPs (inset in Figure 2C). The EDS spectrum demonstrated that the as-grown NPs are made of Cu and O only and the atomic ratio of Cu and O is approximately 1:1 (Figure 2D). The observed diffraction peaks of XRD (Figure 2E) are characteristics of monoclinic phase of CuO (JCPDS 05-0661).[26,27] Except the characteristic CuO peaks, no peaks for other impurities or other crystal phases such as Cu_2O and $Cu(OH)_2$ were observed, which confirms that the as-grown CuO NPs are high purity crystalline. According to the Scherrer equation the average size of CuO NPs is estimated to be ∼5 nm, which is in good agreement with the observed TEM images. To determine the optical properties of CuO NPs, the Raman-scattering measurements were carried out at room temperature with the 514.5 nm line of the Ar^+ laser as the excitation source (Figure 2F). Generally, CuO belongs to the C_{2h}^6 space group with two molecules per primitive cell. There are 12 zone-center optical phonon modes with symmetries $4A_u + 5B_u + A_g + 2B_g$ but only three are ($A_g + 2B_g$) Raman active.[28] The presence of a broad and strong peak at 274 cm^{-1} corresponds to A_g mode and comparatively low-intensity peaks at 324 and 604 cm^{-1} correspond to B_g mode. Noteworthy, these wavenumbers are lower than previous studies, that is, 298, 345, and 632 cm^{-1}, which is attributed to size effect of CuO NPs. Xu et al. demonstrated that with a decrease in particles size, the Raman peaks shifts toward the lower wavenumber as a result of the quantum confinement effect (i.e size effect) and vice versa.[28]

As far growth of CuO NPs is concerned, we observed that presence of acetic acid and addition of NaOH at heating temperature play an important role in the formation of such a small size CuO NPs. Generally, addition of NaOH in copper precursor solution at room temperature with further heating temperature at 90−100 °C leads to the formation of CuO petal-like structure instead of CuO NPs because at this condition the nucleation and growth rate of CuO particles were low.[29] On the other hand if NaOH was added in the boiling solution with the presence of acetic acid, higher temperature caused higher reaction rate with generating large amount of nuclei in a very short time, leads to the formation of small size nanoparticles.

dx.doi.org/10.1021/ac402925r | Anal. Chem. 2013, 85, 10448−10454

Inkjet Printing of CuO NPs Based Ink on the Electrode. The as-formulated ink was vertically dropped from the nozzle with drop-spacing (DS) of 35 μm and due to merging phenomenon between dots resulted interconnected printed film on the Si/Ag substrate. We have also checked the applicability of as-formulated CuO ink and measured contact angles by dropping the CuO ink on Si/Ag substrate. From the contact angle measurement, a low contact angle value of ~28.770 was observed. Low contact angle value is important for good wettability of ink on substrate and also surface energy of the substrate must be higher than the surface tension of the liquid to make uniform film morphology. Further, for the utilization of CuO NPs ink in sensor application, 2 × 2 mm^2 size square-pattern was directly printed on electrode surface. As-printed CuO film was then employed for 2 min microwave-assisted annealing (MAA) before final sensor setup. Figure 3A shows surface FESEM image of printed CuO NPs after MAA treatment. It is clearly seen that as-printed film possessed interconnected porous morphology and the overprinted film showed the uniform thicknesses of ~615 nm (Figure 3B). The printed square pattern (annealed for 2 min) shows a smooth surface topography in 1 × 1 μm^2 area with root-mean-square (rms) roughness of 5.21 nm with interconnected 3-dimensional nanofilms without any structural defects (Figure 3C, D). It is worthwhile to note that printed square-pattern with CuO ink did not show any defects such as coffee-ring effect or bulging. It was also observed that the as-printed film showed good fixation between ink and substrate.

Cyclic Voltammetry of Glucose at the Si/Ag/CuO NPs Electrode. The cyclic voltammograms (CVs) of the Si/Ag/CuO NPs electrode and the Si/Ag electrode were conducted in 0.10 M NaOH solution in the presence and absence of glucose, respectively. A small current was observed at the Si/Ag/CuO NPs electrodes in 0.10 M NaOH solution, while a dramatic increase of current signal toward the positive end of the potential range was observed when the Ag/CuO NPs electrode was used with 2.0 mM glucose, where the oxidation process starts at approximately +0.40 V with broad peak at around +0.60 V (Figure 4). But, no obvious redox activity is observed at the Si/Ag electrode over most of the potential range in 0.10 M NaOH solution. This indicates that inkjet printed CuO NPs greatly improves the performance of the electrode, which is attributed to the large surface area, high surface energy, and enhanced electron transfer of CuO NPs. To study the fouling behavior of this modified electrode, the CVs were performed in 0.10 M NaOH solution, with and without bubbling nitrogen in solution with 2.0 mM glucose. It was observed that the glucose oxidative peak current did not change in both the cases, indicating that oxygen was not involved in this reaction and direct oxidation of glucose contributed to the observed current.

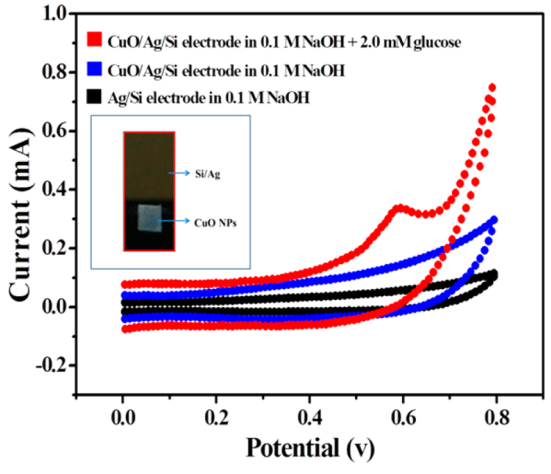

Figure 4. CVs of CuO NPs modified electrode in 2.0 mM glucose (red), without glucose (blue), and bare electrode (black) at scan rate of 100 mV/s in 0.10 M NaOH. Inset shows the sensor image.

To date, the exact mechanism for oxidation of glucose on the CuO modified electrode in an alkaline medium is still under debate. However, from the previous works the most accepted oxidation mechanism of glucose on the modified copper-based electrodes was first suggested by Marioli and Kuwana[30] and later by Wei et al.[31] Where, the oxidation is generated by the deprotonation of glucose and isomerization to its enediol form, followed by adsorption onto the electrode surface and oxidation by Cu(II) and Cu(III). Glucose oxidation occurred at a potential range of 0.40−0.80 V, where the oxidation wave for Cu(II)/Cu(III) was demonstrated.[32,33,41] Herein, the Cu(III) species are proposed to act as an electron-transfer medium.[34,50] The possible reaction could be explained by the following equations:[35]

$$CuO + OH^- \rightarrow CuOOH + e^- \quad \text{(i)}$$

$$CuOOH + e^- + \text{glucose} \rightarrow CuO + OH^- + \text{gluconic acid} \quad \text{(ii)}$$

During cyclic voltammetric measurement, Cu(II) on a CuO electrode would be first oxidized to Cu(III) i. Then the oxidative Cu(III) could catalyze glucose oxidation to generate gluconolactone and then gluconolactone is further oxidized to glucose acid ii. Where, the reaction catalyzed by CuO in the electrochemical nonenzymatic detection of glucose reduction is assisted by the Cu(II)/Cu(III) redox couple. Thus, an enhanced catalytic current response on our CuO modified electrode in the presence of glucose solution and the response current depends on the glucose concentration.

Amperometric Performance of the Si/Ag/CuO NPs Electrode to Glucose. The performance of the sensor has been investigated under different glucose concentration solutions. Figure 5A shows amperometric response of Si/Ag/CuO NPs modified electrode on the successive addition of glucose into continuously stirred 0.10 M NaOH solution at a working potential of +0.60 V. The modified electrode exhibits a rapid and sensitive response to change of glucose concentration and an obvious increase in current upon successive addition of glucose. The modified electrode also achieved 97% steady state current within <2 s. This indicates a good electrocatalytic oxidative and fast electron conduction behavior of the modified electrode. Following the increase of the glucose concentration, response current increases and saturates at a high concentration of glucose, suggesting the saturation of electrocatalytic active sites of CuO NPs. Each experiment was performed three times and the average response of the sensor was calibrated in a wide concentration range with the relative standard deviations of measurements. The calibration curve of the nonenzymatic glucose sensor based on inkjet-printed CuO NPs is shown in Figure 4B. The linear range of the calibration curve is from 0.05 to 18.45 mM (correction coefficient R = 0.9987), with a detection limit of ~0.5 μM at the signal-to-noise ratio (S/N) of 3 for glucose. The sensitivity of the inkjet printed CuO NPs based sensor is 2762.5 $\mu A\ mM^{-1}\ cm^{-2}$. Compared with other CuO nanostructures modified electrochemical sensors for

dx.doi.org/10.1021/ac402925r | Anal. Chem. 2013, 85, 10448−10454

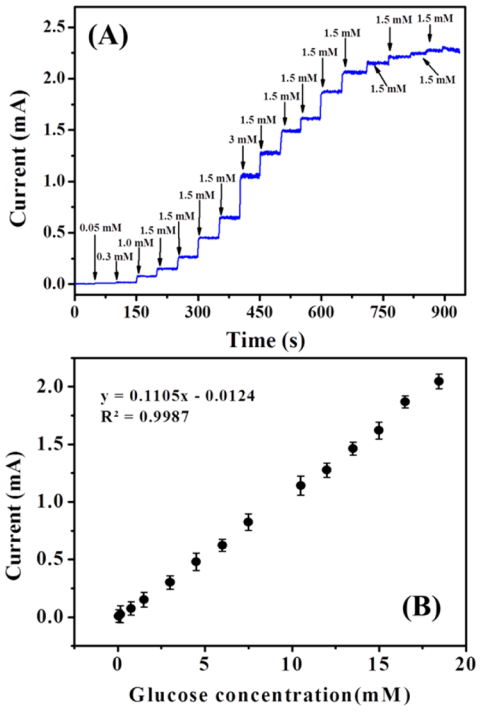

Figure 5. (A) Steady-state current−time responses of glucose at the CuO NPs modified Si/Ag electrode at +0.60 V in 0.10 M NaOH. (B) The calibration curve (current vs concentration) of glucose. Error bars indicate standard deviations of three measurements.

glucose detection (Table 1), the sensitivity of inkjet printed CuO NPs based sensor is indeed lower than the CuO nanoplatelets/Cu foil[45] and sandwich structured CuO/GCE electrode,[48] but the sensitivity and linear range are superior to most of the sensors.[36−44,46,47,49−51] The high sensitivity and the wide linear range of inkjet printed CuO NPs based sensor are mainly attributed to two aspects: the porous nature and the tight adhesion of inkjet-printed CuO NPs on the surface of electrode. The former provides the higher specific surface area and latter enables fast and direct conduction of electron between NPs and Ag electrodes, resulting in faster response and higher sensitivity. In this work, the low detection limit obtained will allow this sensor to be used for noninvasive detection of glucose in other biological fluids (urine, saliva, and sweat) where glucose is too low.

Anti-interference Ability, Stability, and Reproducibility. Generally in the human blood, the interfering species concentration is approximately 30 to 50 times less than that of glucose. Therefore, both lower and higher concentrations of the interferants were employed to evaluate the selectivity of the Si/Ag/CuO NPs sensor by CV and amperometric measurements. As shown in the Figure 6A, CV response of the CuO NPs modified electrode in 1.0 mM glucose without and with low concentration of interfering species (AA, UA, DA, lactose, fructose, and mannose) is almost similar. However, a minor increase in CV response was noticed in the presence of high concentration of interfering species. Similarly, anti-interference ability of the sensor is also evaluated by amperometric measurements after addition of 1.0 mM glucose and subsequent low concentrations (0.10 mM) of each interfering species such as AA, UA, DA, lactose, fructose, and mannose; followed by successive addition of 1.0 mM glucose and higher concentration (0.50 mM) of above interfering species in 20 mL NaOH (0.10 M) solution at a potential of +0.60 V (vs Ag/AgCl). The well-defined response of the sensor after addition of 1.0 mM glucose and the interfering species effect on the detection of glucose at the CuO NPs modified electrodes are shown in Figure 6B. The addition of low concentration of interferents (glucose/interferents = 10:1), that is, AA, UA, and DA do not show any obvious effect, whereas sugars, that is, lactose, fructose, and mannose shows the current response <1% (% current response with respect to glucose) in the presence of glucose. At higher concentration of interferents (glucose:interferents = 10:5), AA, UA, and DA shows almost negligible impact on glucose detection but sugar derivatives (lactose, fructose and mannose) shows the current response >10%. This confirms that only sugar derivatives are responsible for the slight increase of sensor response in CV measurements. Especially, the low sensitivity of AA, UA, and DA of the

Table 1. Comparison of the Nonenzymatic Sensors Based on CuO Nanostructures Modified Substrate/Electrodes

electrode type	response (s)	linear range (mM)	detection limit (μM)	sensitivity (μA mM^{-1} cm^{-2})	ref
inkjet printed CuO NPs/Ag/Si	<2	0.05−18.45	~0.5	2762.5	this work
CuO-MWCNTs/TA plate	<2	0.2−3.0	0.8	2190	36
CuO nanospheres/GCE		0−2.55	1.0	404.53	37
flower-shaped CuO/graphite	15		4.0	709.52	38
CuO nanorods/graphite	10	0.004−8.0	4.0	371.43	
CuO NWs-NFs/GCE	<2	0.5−0.488 and 0.988−5.488	0.045	64.1	39
CuO-MWCNTs/TA foil	1	0.0004−1.2	0.20	2596	40
CuO NWs/Cu	<1	0.0004−2.0	0.049	490	41
CuO/TiO_2	<4	0−2.0	1.0	79.79	42
CuxO/Cu		0−6.0	49	1620	43
CuO nanoplates/TiO_2	<10	0.01−2.0	0.39	1321	44
CuO nanoplatelets/Cu foil		0−0.80	0.5	3490.7	45
CuO-Tyr/Pt		0.9−16.0	20	9.02	46
CuO/Pt		1.0−5.0		2.09	
CuO-graphene/GCE	1	0.001−8.0	1	1065.21	47
sandwich structured CuO/GCE	~0.7	0−3.20	~1	5342.8	48
Cu-CuO NWs/GCE	<5	0.1−12.0	50	761.9	49
Cu nanocluster/MWCNTs/GCE	5	0.0007−3.50	0.21	253	50
CuO NFs/GCE	1	0.006−2.5	0.8	431.3	51

dx.doi.org/10.1021/ac402925r | Anal. Chem. 2013, 85, 10448−10454

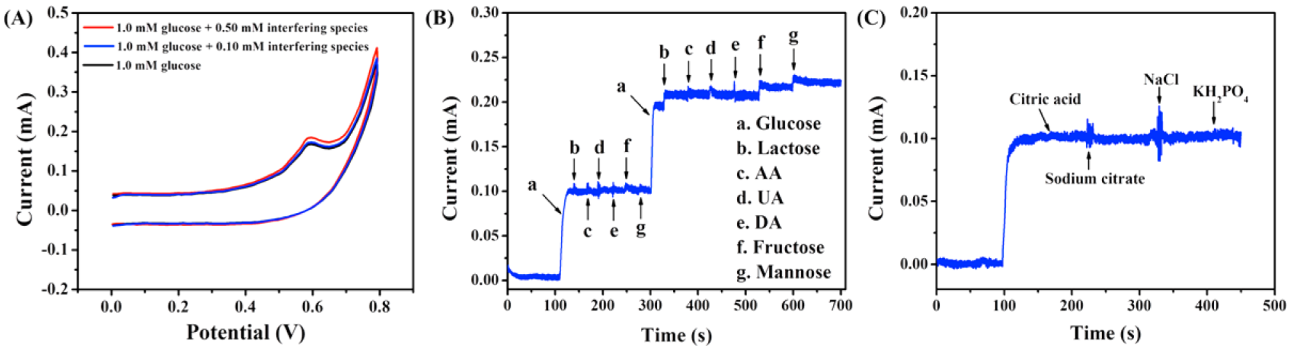

Figure 6. (A) CVs of CuO NPs modified electrode in 1.0 mM glucose without (black-line), with 0.10 mM (blue-line) and 0.50 mM (red-line) interfering species (lactose, AA, UA, DA, fructose, and mannose) at scan rate of 100 mV/s in 0.10 M NaOH. (B) Amperometric responses of the Si/Ag/CuO NPs modified electrode after initial addition of 1.0 mM glucose and 0.10 mM of each interfering species and then again 1.0 mM glucose, followed by addition of higher concentration (0.50 mM) of interfering species (lactose, AA, UA, DA, fructose, and mannose). (C) Chloride poisoning test of the sensor by subsequent addition of 1.0 mM glucose and 0.10 mM of each chloride poisons (citric acid, sodium citrate, NaCl, and KH_2PO_4) in 0.10 M NaOH at an applied potential of +0.60 V (vs Ag/AgCl).

fabricated sensor is attributed to high basic experimental pH condition and high anti-interference ability of inkjet printed CuO NPs electrode. As these species are electroactive at only acidic pH on bare Au and GC electrodes, the increment in response current with increasing pH value reaches at optimum value in acidic pH followed by subsequent decrease with further increased pH.[52,53] However, Ag modified electrode also shows the optimum electrochemical response for AA, DA, and UA at pH = 2.0.[54] Thus, the lower concentration of AA, DA, and UA does not show any response and cause negligible impact on glucose detection. It is concluded from the obtained results and after comparing with previous reported literatures[45,48] that our fabricated sensor shows reliable anti-interference property and are also highly suitable for detection of glucose in real/near real-time samples. The chloride poisoning of the electrodes were also checked by introducing chloride poisons (citric acid, sodium citrate, NaCl, and KH_2PO_4), which shows no significant response (Figure 6C). It suggests that our fabricated electrodes are excellent poison resistance.

The long-term storage stability of electrodes were tested by storing in air at ambient conditions and studying the response intermittently. The activity of Si/Ag/CuO NPs modified electrode nearly had no change within first 60 days and after 90 days the electrodes retains about 95% of its original response to glucose. The reproducibility of the sensor was also evaluated by measuring the response current of four inkjet printed CuO NPs electrode at +0.60 V. The relative standard deviation (RSD) is 2.2%, confirming a good reproducibility of the electrode. The high stability and reproducibility of Si/Ag/CuO NPs electrode in glucose electro-oxidation resulted from the chemical stability of CuO NPs and pore-like structure formed on Ag surface, which prevented the copper-based materials from conglomeration and the interference of oxygen in the air.

Real Sample Analysis. To verify its workability, the sensor was applied to the determination of glucose in human serum samples at 37 °C. The Si/Ag/CuO NPs working electrode with a reference (Ag/AgCl) and counter (Pt) electrodes were immersed in 20 mL of NaOH (0.10 M) solution containing different concentration of human serum samples (diluted from known concentration of glucose in serum sample) at constant potential of +0.60 V, the recovery of glucose was conducted by standard addition of pure glucose to the electrolyte containing serum samples and the determination results were summarized in the Table 2. The data from the proposed glucose sensor are in good agreement with the known concentration of glucose (4.89 mM) in the human serum (Sigma-Aldrich, H4522).[55]

Table 2. Determination of Glucose in Human Serum Samples

samples	concentration (mM)	RSD (%) (n = 3)	added glucose (mM)	recovery (%)
1	1.22	2.3	0.10	94
2	2.45	3.8	0.10	98
3	3.67	2.4	0.10	97

CONCLUSIONS

In summary, we have successfully synthesized CuO NPs via simple solution process. As-synthesized CuO NPs were characterized in detail of its structural and optical properties and found that as-synthesized NPs were grown uniformly with particle size in the range of 5−8 nm. The as-grown NPs showed highly crystalline, pure and stable monoclinic phase of CuO. Moreover, the CuO NPs were further formulated as an ink using mixed solvents of water, ethanol, iso-propanol and diethylene glycol with 20 wt % CuO NPs. As-formulated ink sample was utilized to fabricate a new nonenzymatic glucose sensor based on inkjet printed Si/Ag/CuO NPs electrode. It is observed that microwave-assisted annealing produces smooth surface with interconnected 3-dimensional nanofilms on Ag/Si electrode without any structural defects. The fabricated sensor presents a number of attractive analytical features such as high sensitivity, good stability, reproducibility, selectivity, and wide linear range as well as fast response time. The data from glucose determination in blood serum samples are in accordance with the calculated ones. This inkjet printing method can easily be used for the mass-production of electrodes using CuO NPs-ink not only on the Si/Ag electrode but also on the variety of electrodes material to use for long-term as an amperometric sensor for routine analysis of glucose in real blood serum samples as well as in agricultural products or foods.

AUTHOR INFORMATION

Corresponding Author

*Tel.: +82 63 2702439. Fax: +82 63 2702306. E-mail: ybhahn@chonbuk.ac.kr.

Author Contributions

R.A. amd M.V. contributed equally to this work.

Notes

The authors declare no competing financial interest.

■ ACKNOWLEDGMENTS

This work was supported by the Priority Research Centers Program (2009-0094031) through the National Research Foundation (NRF) of Korea funded by Ministry of Education. Authors also thank KBSI, Jeonju branch for SEM analysis, and Mr. Jong-Gyun Kang, Centre for University Research Facility (CURF), for taking good quality TEM images.

■ REFERENCES

(1) Rasooly, A.; Jacobson, J. *Biosens. Bioelectron.* **2006**, *21* (10), 1851−1858.
(2) Wang, J. *Chem. Rev.* **2008**, *108* (2), 814−825.
(3) Lee, M.-C.; Kabilan, S.; Hussain, A.; Yang, X.-P.; Blyth, J.; Lowe, C. *Anal. Chem.* **2004**, *76* (19), 5748−5755.
(4) Vaddiraju, S.; Tomazos, I.; Burgess, D. J.; Jain, F. C.; Papadimitrakopoulos, F. *Biosens. Bioelectron.* **2010**, *25* (7), 1553−1565.
(5) Ahmad, R.; Tripathy, N.; Kim, J.-H.; Hahn, Y.-B. *Sens. Actuators B* **2012**, *174*, 195−201.
(6) Hahn, Y.-B.; Ahmad, R.; Tripathy, N. *Chem. Commun.* **2012**, *48* (84), 10369−10385.
(7) Hansen, B. J.; Kouklin, N.; Lu, G.; Lin, I.-K.; Chen, J.; Zhang, X. *J. Phys. Chem. C* **2010**, *114* (6), 2440−2447.
(8) Cao, D.; Wang, C.; Zheng, F.; Dong, W.; Fang, L.; Shen, M. *Nano Lett.* **2012**, *12* (6), 2803−2809.
(9) Teng, F.; Yao, W. Q.; Zheng, Y. F.; Ma, Y. T.; Teng, Y.; Xu, T. G.; Liang, S. H.; Zhu, Y. F. *Sens. Actuators B: Chem.* **2008**, *134* (2), 761−768.
(10) Kim, J.; Kim, W.; Yong, K. *J. Phys. Chem. C* **2012**, *116*, 15682−15691.
(11) Dar, M. A.; Kim, Y. S.; Kim, W. B.; Sohn, J. M.; Shin, H. S. *Appl. Surf. Sci.* **2008**, *254* (22), 7477−7481.
(12) Patil, S. A.; Patil, L. A.; Patil, D. R.; Jain, G. H.; Wagh, M. S. *Sens. Actuators B* **2007**, *123* (1), 233−239.
(13) Gou, X.; Wang, G.; Yang, J.; Park, J.; Wexler, D. *J. Mater. Chem.* **2008**, *18*, 965−969.
(14) Zhu, Y. W.; Yu, T.; Cheong, F. C.; Xu, X. J.; Lim, C. T.; Tan, V. B. C.; Thong, J. T. L.; Sow, C. H. *Nanotechnology* **2005**, *16* (1), 88−92.
(15) Xiang, J. Y.; Tu, J. P.; Huang, X. H.; Yang, Y. Z. *J. Solid State Electrochem.* **2008**, *12* (7−8), 941−954.
(16) Jin, R.-C.; Cao, Y.-W.; Mirkin, C. A.; Kelly, K. L.; Schatz, G. C.; Zheng, J.-G. *Science* **2001**, *294*, 1901−1903.
(17) Si, P.; Huang, Y.; Wang, T.; Ma, J. *RSC Adv.* **2013**, *3*, 3487−3502.
(18) Ahmad, R.; Tripathy, N.; Hahn, Y.-B. *Sens. Actuators B* **2012**, *169*, 382−386.
(19) Ahmad, R.; Tripathy, N.; Hahn, Y.-B. *Biosens. Bioelectron.* **2013**, *45*, 281−286.
(20) Calvert, P. *Chem. Mater.* **2001**, *13* (10), 3299−3305.
(21) Lee, Y.; Choi, J.-R.; Lee, K. J.; Stott, N. E.; Kim, D. *Nanotechnology* **2008**, *19* (41), 415604−415610.
(22) Kosmala, A.; Wright, R.; Zhang, Q.; Kirby, P. *Mater. Chem. Phys.* **2011**, *129* (3), 1075−1080.
(23) Vaseem, M.; Lee, K. M.; Hong, A.-R.; Hahn, Y.-B. *ACS Appl. Mater. Interfaces* **2012**, *4* (6), 3300−3307.
(24) Ko, S. H.; Lee, D.; Hotz, N.; Yeo, J.; Hong, S.; Nam, K. H.; Grigoropoulos, C. P. *Langmuir* **2012**, *28* (10), 4787−4792.
(25) Vaseem, M.; Hong, A.-R.; Kim, R.-T.; Hahn, Y. B. *J. Mater. Chem. C* **2013**, *1*, 2112−2120.
(26) Vaseem, M.; Umar, A.; Kim, S. H.; Al-Hajry, A.; Hahn, Y. B. *Mater. Lett.* **2008**, *62* (10−11), 1659−1662.
(27) Vaseem, M.; Umar, A.; Hahn, Y. B.; Kim, D. H.; Lee, K. S.; Jang, J. S.; Lee, J. S. *Catal. Commun.* **2008**, *10* (1), 11−16.
(28) Xu, J. F.; Ji, W.; Shen, Z. X.; Li, W. S.; Tang, S. H.; Ye, X. R.; Jia, D. Z.; Xin, X. Q. *J. Raman Spectrosc.* **1999**, *30* (5), 413−415.
(29) Vaseem, M.; Umar, A.; Hahn, Y. B. *J. Nanosci. Nanotechnol.* **2008**, *8* (10), 5511−5515.
(30) Marioli, M.; Kuwana, T. *Electrochim. Acta* **1992**, *37* (7), 1187−1197.
(31) Wei, H.; Sun, J.-J.; Guo, L.; Li, X.; Chen, G.-N. *Chem. Commun.* **2009**, *20*, 2842−2844.
(32) Torto, N.; Ruzgas, T.; Gorton, L. *J. Electroanal. Chem.* **1999**, *464* (2), 252−258.
(33) Wang, A. J.; Feng, J. J.; Li, Z. H.; Liao, Q. C.; Wang, Z. Z.; Chen, J. R. *CrystEngComm* **2012**, *14*, 1289−1295.
(34) Paixao, T. R. L. C.; Corbo, D.; Bertotti, M. *Anal. Chim. Acta* **2002**, *472* (1−2), 123−131.
(35) Sun, S.; Zhang, X.; Sun, Y.; Yang, S.; Song, X.; Yang, Z. *Phys. Chem. Chem. Phys.* **2013**, *15*, 10904−10913.
(36) Yang, J.; Jiang, L.-C.; Zhang, W.-D.; Gunasekaran, S. *Talanta* **2010**, *82* (1), 25−33.
(37) Reitz, E.; Jia, W.; Gentile, M.; Wang, Y.; Lei, Y. *Electroanalysis* **2008**, *20* (22), 2482−2486.
(38) Wang, X.; Hu, C.; Liu, H.; Du, G.; He, X.; Xi, Y. *Sens. Actuators B* **2010**, *144*, 220−225.
(39) Zhang, P.; Zhang, L.; Zhao, G.; Feng, F. *Microchim. Acta* **2012**, *176* (3−4), 411−417.
(40) Jiang, L.-C.; Zhang, W.-D. *Biosens. Bioelectron.* **2010**, *25* (6), 1402−1407.
(41) Zhuang, Z.; Su, X.; Yuan, H.; Sun, Q.; Xiao, D.; Choi, M. M. F. *Analyst* **2008**, *133* (1), 126−132.
(42) Luo, L.; Zhu, L.; Wang, Z. *Bioelectrochem.* **2012**, *88*, 156−163.
(43) Li, C.; Su, Y.; Zhang, S.; Lv, X.; Xia, H.; Wang, Y. *Biosens. Bioelectron.* **2010**, *26* (2), 903−907.
(44) Chen, J.; Xu, L.; Xing, R.; Song, J.; Song, H.; Liu, D.; Zhou, J. *Electrochem. Commun.* **2012**, *20*, 75−78.
(45) Wang, J.; Zhang, W.-D. *Electrochim. Acta* **2011**, *56* (22), 7510−7515.
(46) Anu Prathap, M. U.; Kaur, B.; Srivastava, R. *J. Colloid Interface Sci.* **2012**, *370* (1), 144−154.
(47) Hsu, Y.-W.; Hsu, T.-K.; Sun, C.-L.; Nien, Y.-T.; Pu, N.-W.; Ger, M.-D. *Electrochim. Acta* **2010**, *82* (1), 152−157.
(48) Meher, S. K.; Rao, G. R. *Nanoscale* **2013**, *5* (5), 2089−2099.
(49) Wang, G.; Wei, Y.; Zhang, W.; Zhang, X.; Fang, B.; Wang, L. *Microchim. Acta* **2010**, *168*, 87−92.
(50) Kang, X.; Mai, Z.; Zou, X.; Cai, P.; Mo, J. *Anal. Biochem.* **2007**, *363*, 143−150.
(51) Wang, W.; Zhang, L.; Tong, S.; Li, X.; Song, W. *Biosens. Bioelectron.* **2009**, *25*, 708−714.
(52) Lin, X.; Zhang, Y.; Chen, W.; Wu, P. *Sens. Actuators B* **2007**, *122*, 309−314.
(53) Huang, J.; Liu, Y.; Hou, H. *Biosens. Bioelectron.* **2008**, *24* (4), 632−637.
(54) Noroozifar, M.; Khorasani-Motlagh, M.; Taheri, A. *Talanta* **2010**, *80* (5), 1657−1664.
(55) Ammam, M.; Easton, E. B. *Sens. Actuators B* **2011**, *155* (1), 340−346.